Near-Earth heliospheric magnetic field intensity since 1750: 2. Cosmogenic radionuclide reconstructions

M. J. Owens, E. Cliver, K. G. Mccracken, J. Beer, L. Barnard, M. Lockwood, A. Rouillard, D. Passos, P. Riley, I. Usoskin, et al.

AGU PUBLICATIONS

JGR

Journal of Geophysical Research: Space Physics

RESEARCH ARTICLE
10.1002/2016JA022550

This article is a companion to *Owens et al.* [2016] doi:10.1002/2016JA022529.

Key Points:
- Reconstructions of the near-Earth heliospheric magnetic field intensity, *B*, are compared back to 1750
- Cosmogenic radionuclide reconstructions of *B* show reasonable agreement with sunspot- and geomagnetic-based reconstructions
- Solar minimum conditions are particularly well matched, which may allow accurate reconstruction of *B* prior to 1610

Correspondence to:
M. J. Owens,
m.j.owens@reading.ac.uk

Citation:
Owens, M. J., et al. (2016), Near-Earth heliospheric magnetic field intensity since 1750: 2. Cosmogenic radionuclide reconstructions, *J. Geophys. Res. Space Physics*, *121*, 6064–6074, doi:10.1002/2016JA022550.

Received 19 FEB 2016
Accepted 7 JUN 2016
Accepted article online 16 JUN 2016
Published online 14 JUL 2016

Near-Earth heliospheric magnetic field intensity since 1750: 2. Cosmogenic radionuclide reconstructions

M. J. Owens[1], E. Cliver[2,3], K. G. McCracken[4], J. Beer[5], L. Barnard[1], M. Lockwood[1], A. Rouillard[6], D. Passos[7,8,9], P. Riley[10], I. Usoskin[11], and Y.-M. Wang[12]

[1]Space and Atmospheric Electricity Group, Department of Meteorology, University of Reading, Reading, UK, [2]National Solar Observatory, Boulder, Colorado, USA, [3]Space Vehicles Directorate, Air Force Research Laboratory, Kirtland AFB, New Mexico, USA, [4]Woodlands, New South Wales, Australia, [5]Swiss Federal Institute of Aquatic Science and Technology, Dübendorf, Switzerland, [6]IRAP/CNRS/UPS, PEPS, Toulouse, France, [7]CENTRA, Instituto Superior Tecnico, Universidade de Lisboa, Lisboa, Portugal, [8]GRPS, Department de Physique, Universite de Montreal, Montreal, Quebec, Canada, [9]Departamento de Fisica, Universidade do Algarve, Faro, Portugal, [10]Predictive Science, San Diego, California, USA, [11]ReSoLVE Centre of Excellence and Sodankylä Geophysical Observatory, University of Oulu, Oulu, Finland, [12]Space Science Division, Naval Research Laboratory, Washington, District of Columbia, USA

Abstract This is Part 2 of a study of the near-Earth heliospheric magnetic field strength, *B*, since 1750. Part 1 produced composite estimates of *B* from geomagnetic and sunspot data over the period 1750–2013. Sunspot-based reconstructions can be extended back to 1610, but the paleocosmic ray (PCR) record is the only data set capable of providing a record of solar activity on millennial timescales. The process for converting ^{10}Be concentrations measured in ice cores to *B* is more complex than with geomagnetic and sunspot data, and the uncertainties in *B* derived from cosmogenic nuclides (~20% for any individual year) are much larger. Within this level of uncertainty, we find reasonable overall agreement between PCR-based *B* and the geomagnetic- and sunspot number-based series. This agreement was enhanced by excising low values in PCR-based *B* attributed to high-energy solar proton events. Other discordant intervals, with as yet unspecified causes remain included in our analysis. Comparison of 3 year averages centered on sunspot minimum yields reasonable agreement between the three estimates, providing a means to investigate the long-term changes in the heliospheric magnetic field into the past even without a means to remove solar proton events from the records.

1. Introduction

Long-term solar variability has potentially important implications for studies of both space [*Barnard et al.*, 2011; *Usoskin*, 2013] and terrestrial regional and global climate [*Gray et al.*, 2010; *Lockwood*, 2012; *Ineson et al.*, 2015]. As such, the heliospheric magnetic field, HMF [e.g., *Owens and Forsyth*, 2013], is of direct interest to space weather science and forecasting and is a useful proxy for solar magnetism in general. This work provides new understanding and justification of the use of the cosmogenic radionuclide record in paleoclimate studies [*Lockwood*, 2006; *Beer et al.*, 2012]. Part 1 of this series of two papers [*Owens et al.*, 2016] showed that *B*, the intensity of the HMF in near-Earth space, can be reconstructed back more than two centuries using both geomagnetic and sunspot number (SSN) observations with remarkably low uncertainties and considerable agreement between these two independent sources of information of past HMF variations. The composite geomagnetic reconstructions, B[GEO], provide the most accurate method for inferring *B*, both in terms of agreement with direct spacecraft observations and within the two methods adopted. B[GEO] can be reliably extended back to 1845. Sunspot number reconstructions, B[SSN], are obviously highly dependent on the underlying sunspot record, but also, to a lesser extent, on the methodology used to convert SSN to *B*. Nevertheless, a composite of records and techniques produces an extremely good match with B[GEO]. This technique has been extended back to 1750. In principle, this method could be extended back to 1610, though that requires further assessment of the sunspot records prior to 1750, as discussed in Part 1.

It is also possible to reconstruct *B* using cosmogenic radionuclide data [e.g., *Caballero-Lopez et al.*, 2004; *McCracken et al.*, 2004; *Lockwood*, 2006; *McCracken*, 2007; *McCracken and Beer*, 2007; *Steinhilber et al.*, 2010; *Beer et al.*, 2012; *Steinhilber et al.*, 2012; *Usoskin*, 2013]. In general, such reconstructions are expected to be less accurate than B[GEO] and B[SSN], owing to the indirect relation between the measured property and *B*,

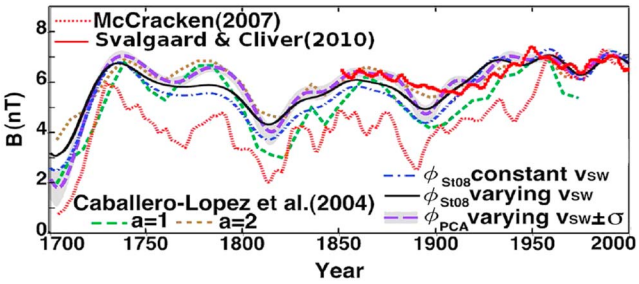

Figure 1. Reconstructions of long-term variations in near-Earth magnetic field intensity, *B*, over the period 1700–2000, adapted from *Svalgaard and Cliver* [2010] and *Steinhilber et al.* [2010]. The solid red line shows a 25 year running mean of the geomagnetic *B* reconstruction from *Svalgaard and Cliver* [2010]. Other curves show cosmogenic radionuclide reconstructions of *B*. They are: 40 year running means (Φ_{St08}, blue and black lines) and 25 year running means (Φ_{PCA}, purple line) from different heliospheric modulation potential estimates provided by *Steinhilber et al.* [2010]; 22 year running means of *Caballero-Lopez et al.* [2004] estimates (green and gold lines); 11 year running means of the *McCracken* [2007] estimate.

as well as the inherent noise in the measurement itself. That indirectness arises from the fact that there are other influences on the cosmic ray flux at Earth and because the near-Earth HMF is a local measure of the heliosphere whereas the external source of cosmic rays means they are influenced by the heliosphere as a whole. Nevertheless, cosmogenic radionuclide reconstructions are invaluable for two reasons. First, they provide the potential to give independent verification of *B* reconstructions over the last 200–400 years. Second, and most importantly, they are the only tool available to study the evolution of the solar wind prior to 1610 and over the previous millennia.

Figure 1, adapted from *Svalgaard and Cliver* [2010] and *Steinhilber et al.* [2010], shows a comparison of the long-term variations in *B* from a geomagnetic reconstruction (solid red line) and cosmogenic radionuclide reconstructions, shown as various colored lines described in the figure caption. At the time of these studies, there was reasonable agreement between the different *B* reconstructions, though the geomagnetic reconstructions of *B* tended to show less long-term variation than the cosmogenic radionuclide reconstructions. Similarly, estimates of *B* over the last century based on the sunspot number [*Solanki et al.*, 2000; *Wang et al.*, 2005; *Vieira and Solanki*, 2010] have tended to be lower before ~1950 than recent reconstructions based on geomagnetic data and cosmogenic radionuclide data [see, e.g., *McCracken*, 2007, Figure 5; *Jiang et al.*, 2011, Figure 9]. More recent sunspot-based estimates of *B*, however, show closer agreement with geomagnetic and cosmogenic estimates [*Owens and Lockwood*, 2012; *Lockwood and Owens*, 2014; *Owens et al.*, 2016], primarily as a result of changes to the underlying SSN records.

It is important to emphasize that we should not expect the agreement between the various *B* reconstructions to be perfect. As mentioned above, the spacecraft and geomagnetic data are essentially point measurements of the solar wind in close proximity to Earth, whereas cosmic ray modulation involves the entire heliosphere [e.g., *Jokipii and Wibberenz*, 1998; *Potgieter*, 2013]. Similarly, the sunspot number is a more global measure than just the HMF sampled near Earth. Nevertheless, the anticorrelation between annual averages of solar wind *B* near Earth and cosmic ray intensity [*Cliver et al.*, 2013, Figure 10] is strong enough that we can reasonably expect to use radionuclides as a tool to infer *B*, at least to within some level of uncertainty. Extracting HMF data from these radionuclides, however, is a much more indirect process than inferring them from sunspot or geomagnetic data. The extracted cosmic ray record may be affected by such factors as terrestrial climate effects on the deposition into the reservoirs in which they are measured, geomagnetic field variability, variations in the local interstellar spectrum of cosmic rays, and high-energy solar energetic particle events (sometimes referred to as "solar cosmic rays") [*Usoskin et al.*, 2006; *Webber et al.*, 2007; *Miyake et al.*, 2012; *Bazilevskaya et al.*, 2014; *Güttler et al.*, 2015; *McCracken and Beer*, 2015].

In order to understand the accuracy and limitations of obtaining solar wind parameters from cosmogenic radionuclides as we go back in time, it is necessary to make a detailed comparison between the *B* series derived from sunspots, geomagnetic data, and the cosmogenic radionuclide data for their period of overlap.

2. Comparison With Cosmogenic Radionuclide Reconstructions

2.1. The Origin of the Cosmogenic Data

The cosmic rays reaching Earth are primarily of galactic origin, having been generated in supernova explosions throughout the galaxy [e.g., *Beer et al.*, 2012]. In addition, intense, short-lived bursts of $<$20 GeV/nucleon radiation are produced sporadically by the Sun, usually in association with large solar flares and fast coronal mass ejections [e.g., *Reames*, 1999; *McCracken et al.*, 2012]. Continuous ground-based ionization chamber

measurements of the >4 GeV/nucleon particles began in 1935 [e.g., *Hess and Graziadei*, 1936; *Forbush*, 1937], later superseded by the worldwide neutron monitor (NM) network (sensitive to >1 GeV/nucleon particles) that commenced in 1951 [e.g., *Simpson*, 2000]. These data, and more recent spacecraft data [e.g., *Heber et al.*, 2009], have shown that the cosmic ray intensity at Earth varies strongly throughout the Schwabe cycle. Theoretical studies [*Parker*, 1958; *Potgieter*, 2013] have shown that these variations are a direct and quantifiable consequence of the varying structure and intensity of the heliospheric magnetic field.

Upon entering the atmosphere, galactic cosmic rays (GCR) initiate nuclear reactions that lead to production of the cosmogenic radionuclides, such as ^{10}Be and ^{14}C (half-lives 1.39×10^6 and 5730 years, respectively) [*Beer et al.*, 2012]. These radionuclides are sequestered in ice cores (^{10}Be) and tree rings (^{14}C). Continuous records of the concentrations of these radioisotopes in their host reservoirs exist for >10,000 years in the past. Following the pioneering work of *Masarik and Beer* [1999], numerical models of cosmogenic radionuclide production, storage, and release have been developed [e.g., *Webber and Higbie*, 2003; *Webber et al.*, 2007; *Kovaltsov and Usoskin*, 2010; *Kovaltsov et al.*, 2012] making it possible to relate these observations quantitatively to the cosmic radiation intensity at Earth. Thus, the cosmogenic data, frequently referred to as paleocosmic ray (PCR) data, yield indirect measurements of the cosmic ray intensity, providing a detailed record of the variability of the GCR intensity at Earth, and solar activity, for >10,000 years into the past [*McCracken et al.*, 2013]. Due to storage and exchange in the oceans and biomass, ^{14}C production changes are strongly damped, which makes resolving individual solar cycles difficult. At the present time there are only two PCR records providing annual measurements covering the interval 1389–1994; ^{10}Be concentrations measured in ice cores from Dye 3 (Greenland) and the North Greenland Ice Core Project (North GRIP). Both are used in this study. It is important to note that the statistical variations in the annual cosmogenic data are much greater than those in the NM data in that the standard deviation of an individual yearly average of the ^{10}Be concentration is ~20%, compared to <0.1% for NM data [*McCracken et al.*, 2004]. While there is limited likelihood of the discovery/utilization of substantial amounts of additional geomagnetic and sunspot data as used in Part 1, there are several new prospective ice cores that will significantly improve the statistical accuracy of the PCR record and the estimates of the HMF derived therefrom. Accordingly, it can be expected that the quality of the PCR record and subsequent reconstructions of *B* will improve considerably over the next decade (see section 2.5).

Unfortunately, use of ^{14}C is made more difficult for the modern period (from about 1850) due to the increasing influence of burning of fossil fuel releasing of "old" carbon into the atmosphere (the so-called First Suess Effect) [*Tans et al.*, 1979] and the atmospheric nuclear bomb tests commencing in the early 1950s. Both significantly alter the atmospheric ^{14}C/^{12}C and ^{13}C/^{12}C ratios, making it difficult to extract the cosmogenic production signal, though recent reconstructions are in broad agreement over the last 400 years [e.g., *Roth and Joos*, 2013; Muscheler et al., The revised sunspot number series in comparison to cosmogenic radionuclide based solar activity reconstructions, submitted to *Solar Physics*, 2016].

2.2. Estimation of the HMF From the Paleocosmic Ray Data

As outlined above, the PCR and instrumental records provide the output of a "heliospheric magnetometer." Using a three-dimensional model of the heliosphere that included a solar cycle-dependent current sheet, latitude dependent solar wind velocities, and the Hale cycle of solar magnetic fields, *Caballero-Lopez et al.* [2004] developed the means to use the annual PCR record to estimate the HMF intensity near Earth. Henceforth, we refer to this as B[GCR]. *McCracken* [2007] modified this method, using the annual NM and Dye 3 records to calibrate the inversion process to the satellite observations of HMF intensity since 1965. Subsequently, a second annual record 1389–1994 (North GRIP) was published [*Berggren et al.*, 2009] and detailed analysis made of the long-term changes in the cosmogenic data using all the available ^{10}Be and ^{14}C data [*Steinhilber et al.*, 2012]. One goal of the ISSI workshop discussed in Part 1 was to use both of these recent advances to update the earlier annual estimates of B[GCR] which were based on an experimental ice core from Dye 3 alone and to compare them with B[GEO] and B[SSN].

To this end, *McCracken and Beer* [2015] combined the Dye 3 and North GRIP ^{10}Be data, reduced climatic and other terrestrial effects using the composite result of *Steinhilber et al.* [2012], and estimated B[GCR] and expected equivalent neutron monitor count rates, dubbed the "pseudo-NM" data, for 1391–1983. Figure 2 a displays the ^{10}Be concentration for the interval 1400–1983; note it was substantially elevated during the Maunder (~1695) and Dalton (~1815) "Grand Minima" in the past. Tables of these annual data together with annual estimates of the HMF (see section 2.3 below) are given in *McCracken and Beer* [2015].

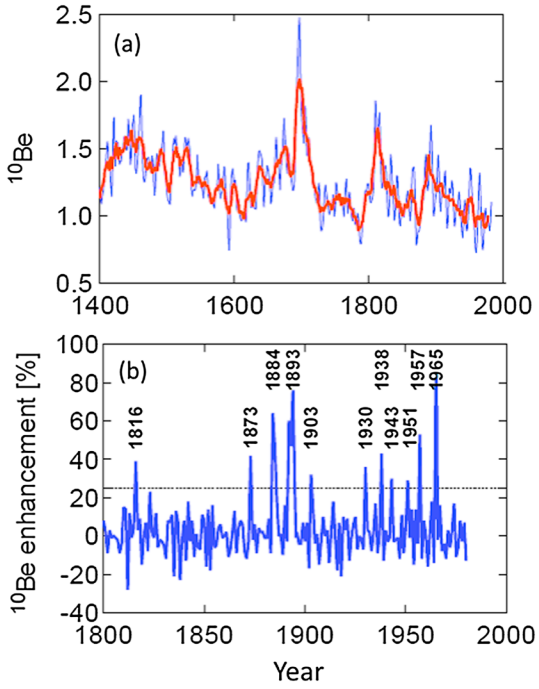

Figure 2. ^{10}Be measurements from ice cores. Figure adapted from *McCracken and Beer* [2015]. (a) Blue: The ^{10}Be concentration, normalized to the average for 1944–1987, after passing through a 1,4,6,4,1 binomial filter. Red: 11 year running means. (b) The impulsive increases in cosmogenic ^{10}Be attributed to solar energetic particles, 1800–1983, which were excised to yield the B[GCR-MB2] estimate of the HMF. The dashed line indicated the 3 standard deviation level.

By comparing individual ice core data, *McCracken and Beer* [2015] also demonstrated the existence of eleven impulsive enhancements (>3 standard deviations) in the annual ^{10}Be data in the interval 1800–1983 as shown in Figure 2b. They further showed that three of these were associated with the energetic particles from the Sun that produced ground-level cosmic ray events in instruments in 1942, 1949, and 1956 (so-called ground-level enhancements, GLEs) and high-altitude nuclear tests in late 1962. Note that the dates do not agree exactly, owing to the 1–2 years deposition time of ^{10}Be from the atmosphere to the ice sheets. Each of the eleven impulsive increases in ^{10}Be in Figure 2b will masquerade as a 3–4 nT decrease in annual values of B[GCR]. Six of the seven impulsive ^{10}Be events in the interval 1800–1942 followed major geomagnetic storms. As major storms are often also accompanied by solar energetic particle (SEP) events (e.g., 16 of the 18 *Dst* <-200 nT storms identified by *Zhang et al.* [2007] are associated with SEPs identified by *Cane et al.* [2010]), *McCracken and Beer* [2015] postulated that these seven impulsive enhancements in ^{10}Be were also of solar origin. On that basis, they excised all >3 standard deviation impulsive enhancements from the ^{10}Be record and used the revised record to estimate the HMF intensity near Earth. We refer to these two different estimates B[GCR-MB1] and B[GCR-MB2]: the former including the solar energetic particle events and the latter after their removal. In the next section, we compare both estimates with B[GEO] and B[SSN] for the interval 1800–1983.

McCracken and Beer [2015] discussed the possibility that the ^{10}Be record may also contain impulsive anomalies associated with volcanic eruptions. Volcanic ejecta do not contain ^{10}Be; however, SO_2 and aerosols therein may influence the atmospheric transportation process. This may accelerate or decelerate the sequestration process, however, no Earth system process, other than GCR spallation of the atmosphere, is known to lead to a net increase in ^{10}Be at this time. *Sigl et al.* [2014] have provided detailed records of the sulfate production by volcanoes during the period of study herein, and further consideration of this putative enhancement processes may be warranted as our physical understanding develops.

An independent estimate of annual B[GCR] is produced using the same data set of ^{10}Be series from the Dye 3 and North GRIP Greenland ice cores but using a slightly different method for converting to *B*. It follows the lower time resolution open solar flux estimate used in *Usoskin et al.* [2015]. First, using the ^{10}Be production model [*Kovaltsov and Usoskin*, 2010] and the most up-to-date geomagnetic field model (the International Geomagnetic Reference Field, IGRF, since 1900 and [*Licht et al.*, 2013] before 1900), the modulation potential, ϕ, was evaluated for each ^{10}Be record. ϕ, effectively a measure of the average rigidity loss of GCR particles in the heliosphere [e.g., *Usoskin*, 2013], was then converted into the open solar magnetic flux [*Usoskin et al.*, 2002; *Alanko-Huotari et al.*, 2006] and ultimately into B[GCR] using the method of *Lockwood et al.* [2014]. The mean of the two resulting B[GCR] estimates from the two ice cores yields the final data sequence used in this study, referred to as B[GCR-U]. It is similar to B[GCR-MB1] in the sense that GLE events were not excluded, e.g., both exhibit very low values in the vicinity of 1893. However, while B[GCR-MB1] and B[GCR-MB2] use

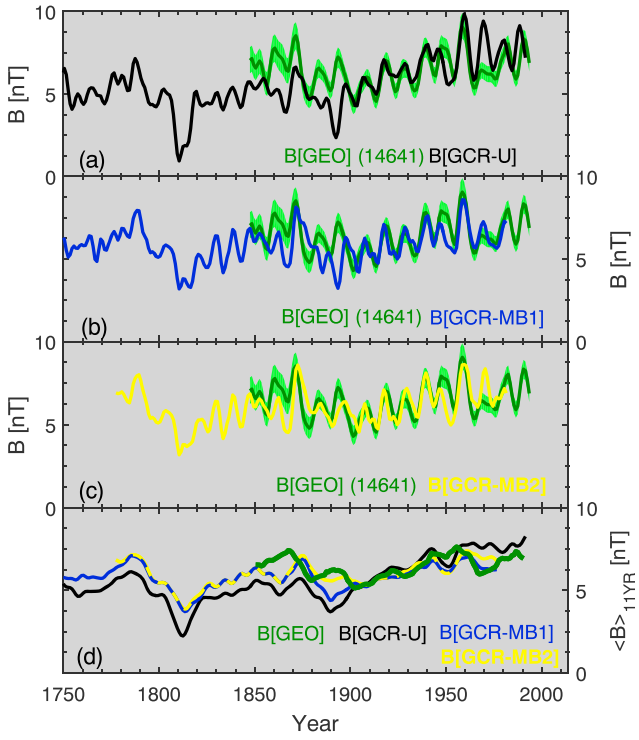

Figure 3. Comparison of geomagnetic and cosmogenic radionuclide reconstructions of *B* over the period 1750–2013. (a–c) The green lines show the annual B[GEO] composite, passed through a 1,4,6,4,1 binomial filter. The green-shaded area shows the 90% confidence interval. The black line in Figure 3a shows B[GCR-U], the ^{10}Be reconstruction of *B* from Usoskin. The dark blue line in Figure 3b shows B[GCR-MB1], the ^{10}Be reconstruction of *B* from *McCracken and Beer* [2015]. The yellow line in Figure 3c shows B[GCR-MB2], the *McCracken and Beer* [2015] estimate with impulsive ^{10}Be enhancements removed. (d) The 11 year running means of the annual data in the same format, with yellow/blue dashed lines indicating 11 year means of B[GCR-MB1] and B[GCR-MB2] when they have the same value.

the results of *Steinhilber et al.* [2012] to minimize the possible effects of long-term climate change and other terrestrial effects in the ^{10}Be data, no allowance was made for these in B[GCR-U]. Therefore, the difference between these estimates serves as an estimate of the model uncertainties and the role of climate effects.

2.3. Comparison of B[GEO], B[SSN], and B[GCR]

Figure 3 compares the geomagnetic *B* reconstruction, B[GEO], in green, with the three B[GCR] estimates (Figures 3a–3c show B[GCR-U], B[GCR-MB1], and B[GCR-MB2] as black, blue, and yellow lines, respectively) for the interval 1750–2005. The B[GCR-MB2] estimate only extends to 1777 as multiple annual resolution ice cores are required to identify SEP-induced ^{10}Be enhancements. All time series (including B[GEO] and B[SSN]) have been passed through a 1,4,6,4,1 binomial filter [*Aubury and Luk*, 1996] to remove the high-amplitude variations due to the 20% standard deviation variability of the annual ^{10}Be data. A 1 year lag has been subtracted from B[GCR] to allow for the deposition of the ^{10}Be from the atmosphere to the polar ice sheet [e.g., *Usoskin*, 2013, and references therein]. Figure 3d shows 11 year means of the annual time series, in the same format (with blue/yellow dashed lines showing times when B[GCR-MB1] and B[GCR-MB2] produce the same 11 year mean value). Figure 4 shows comparisons of B[SSN] (red) with B[GCR] in the same format.

Table 1 compares the linear correlation coefficients (*r*) and mean square errors (MSE) between the three estimates of B[GCR] and the B[GEO] and B[SSN] composites. (Correlation coefficients are all significant at the 90% level, though differences between correlation coefficients, using a Fisher *r*-to-*z* transformation, are not.)

While the long-term trend and 11 year cycles in the three B[GCR] estimates are in reasonable agreement with those of B[GEO] and B[SSN], there are a number of striking differences. B[GCR-U] is significantly lower than and B[GEO] and B[SSN] prior to ~1900. This could suggest that the minimisation of climate and other terrestrial effects incorporated into B[GCR-MB1] and B[GCR-MB2] are important in the *B* reconstruction. The B[GCR-U] underestimate, however, could also be related to the details of how the global measure of open solar flux has been converted to near-Earth *B*. Further investigation is required. In particular, the inclusion of Antarctic ice cores may help assess the role of ^{10}Be deposition.

Note the very low values of both B[GCR-U] and B[GCR-MB1] centered on ~1860–1863, ~1884, ~1893, and ~1948, all four being close to sunspot maximum. These low values are not readily explicable in terms of our modern knowledge of the variation of the HMF during the Schwabe cycle but are consistent with the hypothesis that they are the consequence of GLEs produced by the active Sun; GLEs elevate ^{10}Be production, which is misinterpreted as enhanced GCR intensity resulting from a weaker HMF. Figures 3c and 4c display a comparison of B[GCR-MB2] with B[GEO] and B[SSN], respectively. Examination shows that the two major discrepancies between B[GEO] and B[GCR-MB1] in ~1884 and ~1893 are substantially reduced in B[GCR-MB2],

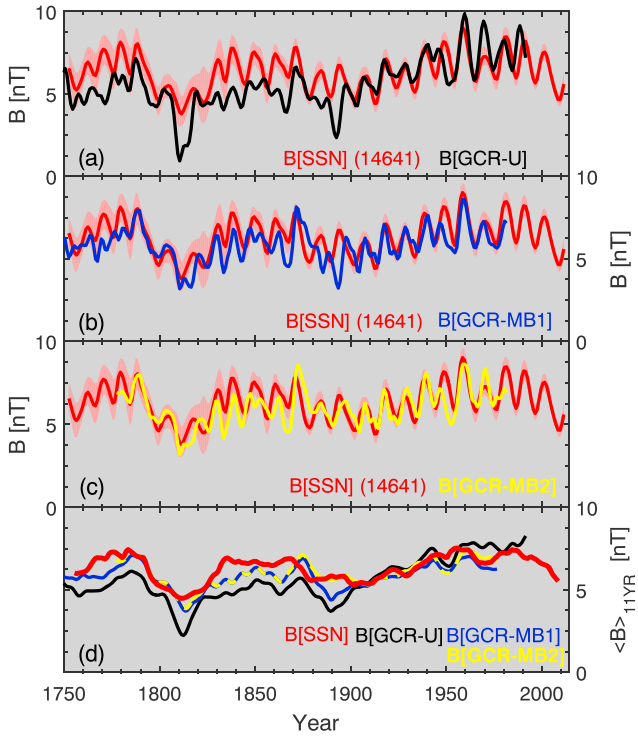

Figure 4. Comparison of the annual B[SSN] composite (red) with cosmogenic radionuclide reconstructions of *B*, in the same format as Figure 3.

as are the smaller effects due to the GLE of 1942, 1949, and 1956, and the nuclear weapon event of 1962. However there are no significant changes in the discrepancies with B[GEO] and B[SSN] for ~1860–1863 and the first two years of the 1948–1952 discrepancy. *McCracken and Beer* [2015] examined the B[GCR-MB2] underestimate at 1948 and concluded that it was due to the production of ^{10}Be by the large, long duration GLE that was observed with ionization chambers on 25 July 1946 [*Forbush*, 1946]. Their analysis shows that the resulting impulsive ^{10}Be enhancement merged with the rapidly falling onset of the 11 year modulation of the galactic cosmic radiation (1946–1948), with the result that the impulsive enhancement was not statistically significant in the annual PCR record (Figure 2b). They concluded that large GLEs occurring during the steep rise in *B* during the ascending phase (typically the second or third year) of a Schwabe cycle may escape detection in this manner in the present-day PCR record. For example, the large discrepancy in the interval 1860–1865 in Figures 3c and 4c may be the consequence of solar energetic particle production during Schwabe cycle 10, 1857–1867 (the Carrington white light flare occurred in 1859). Thus, while *Usoskin and Kovaltsov* [2012] noted the absence of an impulsive ^{10}Be enhancement corresponding to the Carrington flare, *McCracken and Beer* [2015] speculate that this could be a consequence of the superposition effect described above. *McCracken and Beer* [2015] estimate that ~15% of all large GLEs may escape detection in the present-day PCR record in this manner. The inability to detect some large solar energetic particle enhancements appears to be a fundamental but temporary limitation to the estimation of B[GCR] (see section 2.5).

GLEs are rarely observed to occur within ±1 year of sunspot minimum. Figure 5 and Table 2 compare B[GCR], B[GEO] and B[SSN] values for 3 year means centered on sunspot minimum, as defined in *Owens et al.* [2011]. A 3 year mean is used to incorporate the uncertainty in both solar minimum timing and ^{10}Be deposition, though the results are similar for analysis of a single year. The 1845–1983 interval which is covered by B[GEO]

Table 1. Comparison of the B[GEO] and B[SSN] Composites With B[GCR], Cosmogenic Radionuclide Reconstructions of *B*[a]

	B[GCR-MB1]	B[GCR-MB2]	B[GCR-U]
	1846–1983 (N = 137)		
B[GEO]	$r = 0.49$; MSE = 1.3 nT^2	$r = 0.54$; MSE = 1.1 nT^2	$r = 0.39$; MSE = 2.2 nT^2
B[GEO] 14641	$r = 0.53$; MSE = 1.1 nT^2	$r = 0.57$ MSE = 0.85 nT^2	$r = 0.42$; MSE = 2.0 nT^2
B[SSN]	$r = 0.58$; MSE = 1.1 nT^2	$r = 0.63$; MSE = 0.86 nT^2	$r = 0.56$; MSE = 1.6 nT^2
B[SSN] 14641	$r = 0.60$; MSE = 0.94 nT^2	$r = 0.65$; MSE = 0.70 nT^2	$r = 0.59$; MSE = 1.5 nT^2
	1777–1983 (N = 183)		
B[SSN]	$r = 0.67$; MSE = 1.0 nT^2	$r = 0.71$; MSE = 0.81 nT^2	$r = 0.63$; MSE = 1.9 nT^2
B[SSN] 14641	$r = 0.70$; MSE = 0.86 nT^2	$r = 0.73$; MSE = 0.67 nT^2	$r = 0.66$; MSE = 1.8 nT^2

[a]GCR-MB1 and GCR-MB2 refer to McCracken and Beer [2015] estimates, with 1 and 2 representing the nonremoval and removal of impulsive ^{10}Be enhancements, respectively. GCR-U refers to the Usoskin estimate described in the present study. Correlation coefficients and mean square errors are listed for both annual and 1,4,6,4,1 filtered B[GEO] and B[SSN]. Two periods are considered: 1846–1983, the maximum overlap between B[GCR] and B[GEO], and 1777–1983, the maximum overlap between B[GCR] and B[SSN].

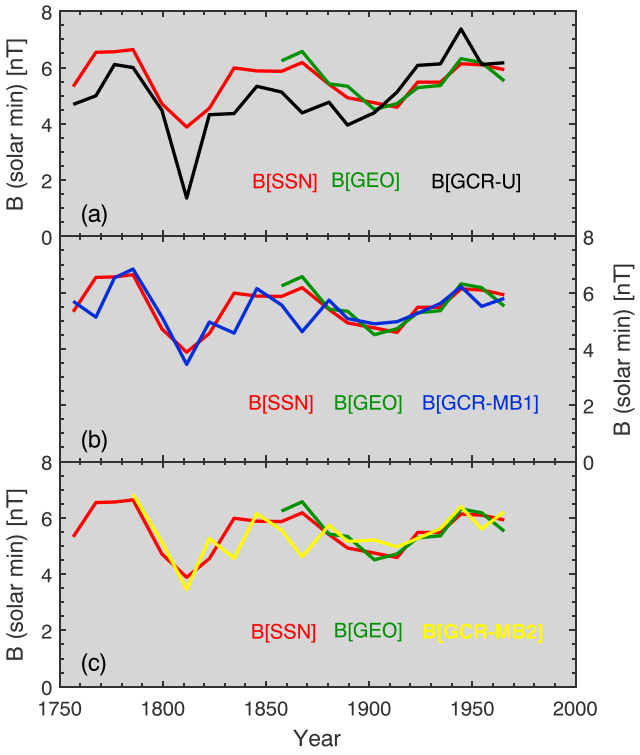

Figure 5. Comparisons of B[GEO], B[SSN], and the three B[GCR] estimates for the 3 year means centered on solar minimum, in the same format as Figures 3 and 4.

does not provide sufficient variability in the solar minimum *B* values to draw strong conclusions. Over the 1777–1983 interval covered by B[SSN], however, there is generally good agreement between B[GCR-MB1] and B[SSN] for the Schwabe minima ($r = 0.69$; MSE = 0.35 nT^2), even without the removal of ^{10}Be enhancements attributed to SEPs. B[GCR-U] shows the same trends as B[SSN] for Schwabe minima, though the long-term variability in B[GCR-U] is much greater than B[SSN], which is reflected in the high correlation ($r = 0.70$) but high MSE (1.0 nT^2). We also note the qualitative agreement between an Antarctic ice core ^{10}Be reconstruction of solar modulation potential [*Muscheler et al.*, 2016] and B[GCR-MB1] for this period.

2.4. Assessment of the Use of B[GCR] Prior to 1750

While we have excellent measurements and theoretical knowledge of the active sun since 1850 primarily through geomagnetic observations, we have few direct observations of the solar "Grand Minima" (e.g., Spoerer 1420–1540; Maunder, 1645–1715; and Dalton 1790–1830). See, e.g., *Riley et al.* [2015] and *Usoskin et al.* [2015] for detailed discussions of the Maunder minimum. The geomagnetic record used to produce B[GEO] only commenced in 1845, although sporadic records are available during the eighteenth century. The cosmogenic estimates of *B* and the sunspot numbers (after 1609) are therefore the only known means to study the heliospheric and solar magnetic effects during the Maunder and earlier Grand Minima. On the basis of the comparisons made in this paper, we now summarize the uncertainties that will arise in the use of the estimates of B[GCR] in such studies.

1. Very large solar energetic particle events, similar to those of 26 July 1946 and 23 February 1956, and especially extreme events like 775 AD [*Miyake et al.*, 2012] which was the greatest documented SEP event over 11 millennia [*Usoskin et al.*, 2013; *Mekhaldi et al.*, 2015] will cause a significant reduction in the annual estimates of *B* based on the cosmogenic data. Provided annual ^{10}Be data are available from two or more ice cores, the largest solar contributions can be identified and removed from the cosmogenic data yielding B[GCR-MB2], except in the ascending phase of the Schwabe cycle. This may result in a $<$1.5 nT underestimate

Table 2. Comparison of the B[GEO] and B[SSN] Composites With B[GCR], Cosmogenic Radionuclide Reconstructions of *B*, for 3 Year Means Centered on Solar Minima[a]

	B[GCR-MB1] (Solar Minima)	B[GCR-MB2] (Solar Minima)	B[GCR-U] (Solar Minima)
	1856–1976 (N = 12)		
B[GEO] (solar minima)	$r = 0.29$; MSE = 0.58 nT^2	$r = 0.20$; MSE = 0.53 nT^2	$r = 0.30$; MSE = 1.0 nT^2
B[SSN] (solar minima)	$r = 0.48$; MSE = 0.28 nT^2	$r = 0.45$; MSE = 0.29 nT^2	$r = 0.51$; MSE = 0.68 nT^2
	1785–1976 (N = 16)		
B[SSN] (solar minima)	$r = 0.69$; MSE = 0.35 nT^2	$r = 0.66$; MSE = 0.38 nT^2	$r = 0.70$; MSE = 1.0 nT^2

[a]GCR-MB1 and GCR-MB2 refer to *McCracken and Beer* [2015] estimates, with 1 and 2 representing the nonremoval and removal of impulsive ^{10}Be enhancements, respectively. GCR-U refers to the Usoskin estimate described in the present study. Two periods are considered: 1856–1976, the maximum period of overlap between B[GEO] and B[GCR], and 1785–1976, the overlap between B[SSN] and B[GCR].

in B[GCR-MB2] after passage through a 1,4,6,4,1 filter for ~15% of all Schwabe cycles. At present, there is no means to compensate for the occurrence of smaller solar events, and this may result in underestimation (<1 nT) of annual B[GCR] near sunspot maximum.

2. There is reasonable agreement between the absolute values of B[GEO], B[SSN], and B[GCR-MB2] throughout the range 4–9 nT. The statistical errors in the cosmogenic data imply a standard error of 0.5 nT for annual estimates of B[GCR-MB2] based upon Dye 3 and North GRIP alone. The difference in the B[GCR-MB1] and B[GCR-U] series, particularly the lower values of B[GCR-U] prior to 1900, may reflect uncertainties related to the corrections for climate effects and the different models used (i.e., numerical Monte-Carlo models of cosmic ray induced cascades, modeling of ^{10}Be transport and deposition, and calibration of the models) and indicates that further work is warranted in this area.
3. Identification of impulsive ^{10}Be enhancements is presently difficult prior to 1760. However, Figure 5 and Table 2 show that the sunspot minimum values of B[GCR-MB1] and B[GCR-U] are well correlated with B[SSN]. Consequently, it will be possible to use Schwabe minimum estimates of B[GCR] to investigate long-term changes in the HMF far into the past. The 40% decreases in the PCR during the Schwabe cycle means that solar minima and maxima are identifiable without difficulty and without reference to a sunspot record. Note, however, that at periods of very low solar activity, it has been postulated on the basis of open solar flux continuity modeling [*Owens and Lockwood*, 2012] that the HMF variation and the solar cycle variation may shift into antiphase [*Owens et al.*, 2012], which could complicate such analysis.
4. There are no direct spacecraft measurements or indirect (B[GEO] or B[SSN]) estimates for annual $B < 3.5$ nT, and therefore, the accuracy of B[GCR-MB2] estimates below this value are dependent wholly upon the applicability of the cosmic ray propagation equation in this parameter regime. This requires further study. Present-day knowledge indicates that the estimates should be reliable for B[GCR-MB2] > 2.5 nT [*McCracken and Beer*, 2015].

2.5. Future Improvements in B[GCR]

The statistical and measurement errors in the PCR data series set the limit on the accuracy of our estimates of B[GCR-MB2] and on our ability to identify solar energetic particle events during the ascending phase of the solar cycle. Improvements in both are possible and might include

1. Increasing the number of annual ^{10}Be records to a total of about five, with two of the new ones coming from the Antarctic. This is particularly important since both ^{10}Be series used here are from Greenland and may be potentially influenced by the regional climate variability [*Usoskin et al.*, 2009; *Beer et al.*, 2012]. The overall goal would be a greater reduction in statistical and systematic noise, and minimization of long-term systematic changes that introduce errors into long-term comparisons. Five independent sets of data would yield a standard deviation of ~5.5% for the annual paleocosmic ray data, 0.3 nT for the annual estimates of the heliospheric magnetic field near Earth, and would allow smaller solar energetic particle events to be detected and eliminated from B[GCR-MB2]. It would also permit the time profile of the 11 year cycle in the PCR to be determined for individual cycles ("sharp rising " or "flat topped") thereby identifying the polarity of the solar dipole into the past [*Potgieter*, 2013; *Owens et al.*, 2015].
2. Extending the annual PCR record back to 1000 before present (B.P.). (950 Common Era (C.E.)) to provide the ability to study the solar, cosmic radiation, and magnetic field effects with annual resolution through the whole cycle of Grand Minima from the Oort (~1040 C.E.) to the Gleissberg (1890 C.E.) Minima.
3. Complementing the ^{10}Be records with records of ^{36}Cl and ^{14}C which are more sensitive to low-energy solar particles and differ in their geochemical properties.
4. Improving the time assignment to ± 1 year and better. A relative error of greater than 1 year between two cores reduces the ability to identify the impulsive ^{10}Be events and thereby reduces the ability to detect and excise SEP events in the past.

3. Discussion and Conclusions

In this paper, we have compared the in situ observations of solar wind *B* with geomagnetic observations, sunspot time series, and the paleocosmic ray record to infer the solar wind magnetic field strength from 1750 to 2013. Our main results are summarized below where, for brevity, we refer to the estimates as B[OBS], B[GEO], B[SSN], and B[GCR], respectively.

1. The original estimates of B[GCR] were based on paleocosmic ray data from a single experimental ice core. Using annual measurements from a second core, and after allowance for experimental uncertainties and long-term changes of atmospheric and geomagnetic origin, *McCracken and Beer* [2015] revised the earlier results upwards to obtain B[GCR-MB1]. Section 2.3 examines the role of very large solar energetic particle events, such as that of 23 February 1956, in introducing significant reductions (~1.5 nT) into the estimates of B[GCR]. The availability of data from two ice cores provides the ability to identify such solar energetic particle events in the past, except during the ascending phase of a solar cycle. *McCracken and Beer* [2015] excised eleven presumed solar energetic particle events from the PCR record, 1800–1980, leading to B[GCR-MB2]. In the 11 year running mean data, there are still two ~1.5 nT excursions below B[GEO], in ~1860–1865 and ~1948, that we speculate are due to the production of solar cosmic rays during the second and third year of the solar cycle and consequently obscured by the rapidly decreasing cosmic ray intensities at those times. An independent estimate of annual B[GCR] based on the work of *Kovaltsov and Usoskin* [2010] and *Usoskin et al.* [2015], termed B[GCR-U], agrees reasonably well with B[GEO], B[SSN], B[GCR-MB1], and B[GCR-MB2] for the twentieth century but falls below those series prior to ~1900. This difference may be due to factors such as climate change or the procedure used to convert open solar flux to near-Earth *B*.
2. Analysis of the interval 1879–1940 shows that there is good agreement between all three estimates B[GEO], B[SSN], and B[GCR-MB2]. The standard deviations of the statistical and measurement errors in annual ^{10}Be data are large (~20%), resulting in standard deviations of ~0.5 nT in the B[GCR] time series. The acquisition of annual ^{10}Be data from three new ice cores would provide enhanced ability to identify and eliminate solar energetic particle contributions in the PCR record and reduction of the standard deviation due to statistical fluctuations to ~0.3 nT. It would also provide the ability to determine the polarity of the solar dipole in the past and to provide insight into the differences between B[GCR] and the other estimates of *B*.
3. There are no direct or indirect measurements via B[GEO] or B[SSN] of $B < 3.5$ nT. Thus, the accuracy of B[GCR-MB2] estimates below this value is entirely dependent on the continued applicability of the cosmic ray propagation equation. Present day knowledge indicates that the estimates will be reliable for $B > 2.5$ nT, though it is important to undertake further study of the propagation equation for low values of *B* in the heliosphere.

Ultimately, studies of the Grand Minima and millennia scale changes in the HMF will be based on the cosmogenic-based estimates, B[GCR]. Their improvement and extension, as discussed in section 2.5, will be crucial for our understanding of such topics as the variability of the solar dynamo and terrestrial climate change.

Acknowledgments

Data are available as supporting information to Part 1 of this study [*Owens et al.*, 2016] and previously published articles cited in the manuscript. This work was partly facilitated by an International Space Science Institute (ISSI) international team selected in 2011 as number 233, "Long-term reconstructions of solar and solar wind parameters" organized by L. Svalgaard, M. Lockwood, and J. Beer. We are grateful to the Space Physics Data Facility (SPDF) and National Space Science Data Center (NSSDC) for the OMNI data. We thank ISSI for supporting the team. M. O., M.L., and L.B. are part funded by Science and Technology Facilities Council (STFC) grant ST/M000885/1. M.O. acknowledges support from the Leverhulme Trust through a Philip Leverhulme Prize. K.G.McC. acknowledges the consistent support he has received since 2005 from the International Space Science Institute, Bern, Switzerland. J.B. acknowledges support from the Swiss National Science Foundation under the grant CRSI122-130642 (FUPSOL) and profited from the PAGES workshops in Davos (2012 and 2014). I.U.'s contribution was made within the framework of the ReSoLVE Centre of Excellence (Academy of Finland, Project 272157). Y.M.W. acknowledges support from the Chief of Naval Research. We thank both referees for useful comments.

References

Alanko-Huotari, K., K. Mursula, I. Usoskin, and G. Kovaltsov (2006), Global heliospheric parameters and cosmic-ray modulation: An empirical relation for the last decades, *Sol. Phys.*, *238*(2), 391–404.

Aubury, M., and W. Luk (1996), Binomial filters, *J. VLSI Signal Proc. Syst. Signal Imag. Video technol.*, *12*(1), 35–50, doi:10.1007/bf00936945.

Barnard, L., M. Lockwood, M. A. Hapgood, M. J. Owens, C. J. Davis, and F. Steinhilber (2011), Predicting space climate change, *Geophys. Res. Lett.*, *38*, L16103, doi:10.1029/2011GL048489.

Bazilevskaya, G. A., E. W. Cliver, G. A. Kovaltsov, A. G. Ling, M. Shea, D. Smart, and I. G. Usoskin (2014), Solar cycle in the heliosphere and cosmic rays, *Space Sci. Rev.*, *186*(1–4), 409–435.

Beer, J., K. G. McCracken, and R. von Steiger (2012), *Cosmogenic Radionuclides: Theory and Applications in the Terrestrial and Space Environments*, Springer, Berlin.

Berggren, A.-M., J. Beer, G. Possnert, A. Aldahan, P. Kubik, M. Christl, S. J. Johnsen, J. Abreu, and B. M. Vinther (2009), A 600-year annual ^{10}Be record from the NGRIP ice core, Greenland, *Geophys. Res. Lett.*, *36*, L11801, doi:10.1029/2009GL038004.

Caballero-Lopez, R. A., H. Moraal, K. G. McCracken, and F. B. McDonald (2004), The heliospheric magnetic field from 850 to 2000 AD inferred from ^{10}Be records, *J. Geophys. Res.*, *109*, A12102, doi:10.1029/2004JA010633.

Cane, H., I. Richardson, and T. Von Rosenvinge (2010), A study of solar energetic particle events of 1997–2006: Their composition and associations, *J. Geophys. Res.*, *115*, A08101, doi:10.1029/2009JA014848.

Cliver, E., I. Richardson, and A. Ling (2013), Solar drivers of 11-yr and long-term cosmic ray modulation, *Space Sci. Rev.*, *176*(1–4), 3–19.

Forbush, S. E. (1937), On the effects in cosmic-ray intensity observed during the recent magnetic storm, *Phys. Rev.*, *51*(12), 1108, doi:10.1103/PhysRev.51.1108.3.

Forbush, S. E. (1946), Three unusual cosmic-ray increases possibly Due to charged particles from the Sun, *Phys. Rev.*, *70*, 771–772, doi:10.1103/PhysRev.70.771.

Gray, L. J., J. Beer, M. Geller, J. D. Haigh, M. Lockwood, K. Matthes, U. Cubasch, D. Fleitmann, G. Harrison, and L. Hood (2010), Solar influences on climate, *Rev. Geophys.*, *48*, RG4001, doi:10.1029/2009RG000282.

Güttler, D., F. Adolphi, J. Beer, N. Bleicher, G. Boswijk, M. Christl, A. Hogg, J. Palmer, C. Vockenhuber, and L. Wacker (2015), Rapid increase in cosmogenic ^{14}C in AD 775 measured in New Zealand kauri trees indicates short-lived increase in ^{14}C production spanning both hemispheres, *Earth Planet. Sci. Lett.*, *411*, 290–297.

Heber, B., A. Kopp, J. Gieseler, H. Fichtner, K. Scherer, M. Potgieter, and S. Ferreira (2009), Modulation of galactic cosmic ray protons and electrons during an unusual solar minimum, *Astrophys. J.*, *699*(2), 1956.
Hess, V. F., and H. T. Graziadei (1936), On the diurnal variation of the cosmic radiation, *Terr. Magn. Atmos. Electr.*, *41*(1), 9–14.
Ineson, S., A. C. Maycock, L. J. Gray, A. A. Scaife, N. J. Dunstone, J. W. Harder, J. R. Knight, M. Lockwood, J. C. Manners, and R. A. Wood (2015), Regional climate impacts of a possible future grand solar minimum, *Nat. Commun.*, *6*, 7535, doi:10.1038/ncomms8535.
Jiang, J., R. H. Cameron, D. Schmitt, and M. Schüssler (2011), The solar magnetic field since 1700-II. Physical reconstruction of total, polar and open flux, *Astron. Astrophys.*, *528*, A83.
Jokipii, J., and G. Wibberenz (1998), Epilogue: Cosmic rays in the active heliosphere, *Space Sci. Rev.*, *83*, 365–368, doi:10.1023/A:1005039410736.
Kovaltsov, G. A., and I. G. Usoskin (2010), A new 3D numerical model of cosmogenic nuclide ^{10}Be production in the atmosphere, *Earth Planet. Sci. Lett.*, *291*, 182–188.
Kovaltsov, G. A., A. Mishev, and I. G. Usoskin (2012), A new model of cosmogenic production of radiocarbon ^{14}C in the atmosphere, *Earth Planet. Sci. Lett.*, *337*, 114–120.
Licht, A., G. Hulot, Y. Gallet, and E. Thébault (2013), Ensembles of low degree archeomagnetic field models for the past three millennia, *Phys. Earth Planet. Int.*, *224*, 38–67.
Lockwood, M. (2006), What do cosmogenic isotopes tell us about past solar forcing of climate?, *Space Sci. Rev.*, *125*, 95–109, doi:10.1007/s11214-006-9049-2.
Lockwood, M. (2012), Solar influence on global and regional climates, *Surv. Geophys.*, *33*(3–4), 503–534, doi:10.1007/s10712-012-9181-3.
Lockwood, M., and M. J. Owens (2014), Centennial variations in sunspot number, open solar flux and streamer belt width: 3. Modeling, *J. Geophys. Res. Space Physics*, *119*, 5193–5209, doi:10.1002/2014JA019973.
Lockwood, M., H. Nevanlinna, L. Barnard, M. Owens, R. Harrison, A. Rouillard, and C. Scott (2014), Reconstruction of geomagnetic activity and near-Earth interplanetary conditions over the past 167 yr–Part 4: Near-Earth solar wind speed, IMF, and open solar flux, *Ann. Geophys.*, *32*(4), 383–399.
Masarik, J., and J. Beer (1999), Simulation of particle fluxes and cosmogenic nuclide production in the Earth's atmosphere, *J. Geophys. Res.*, *104*, 12,099–12,112, doi:10.1029/1998JD200091.
McCracken, K. G. (2007), Heliomagnetic field near Earth, 1428–2005, *J. Geophys. Res.*, *112*, A09106, doi:10.1029/2006JA012119.
McCracken, K. G., and J. Beer (2007), Long-term changes in the cosmic ray intensity at Earth, 1428–2005, *J. Geophys. Res.*, *112*, A10101, doi:10.1029/2006JA012117.
McCracken, K. G., and J. Beer (2015), The Annual Cosmic-radiation Intensities 1391–2014; the annual Heliospheric Magnetic Field Strengths 1391–1983; and identification of solar cosmic ray events in the cosmogenic record 1800–1983, *Sol. Phys.*, *290*(10), 3051–3069, doi:10.1007/s11207-015-0777-x.
McCracken, K. G., F. B. McDonald, J. Beer, G. Raisbeck, and F. Yiou (2004), A phenomenological study of the long-term cosmic ray modulation, 850–1958 AD, *J. Geophys. Res.*, *109*, A12103, doi:10.1029/2004JA010685.
McCracken, K., H. Moraal, and M. Shea (2012), The high-energy impulsive ground-level enhancement, *Astrophys. J.*, *761*(2), 101–113, doi:10.1088/0004-637X/761/2/101.
McCracken, K., J. Beer, F. Steinhilber, and J. Abreu (2013), A phenomenological study of the cosmic ray variations over the past 9400 years, and their implications regarding solar activity and the solar dynamo, *Sol. Phys.*, *286*(2), 609–627, doi:10.1007/s11207-013-0265-0.
Mekhaldi, F., R. Muscheler, F. Adolphi, A. Aldahan, J. Beer, J. R. McConnell, G. Possnert, M. Sigl, A. Svensson, and H.-A. Synal (2015), Multiradionuclide evidence for the solar origin of the cosmic-ray events of AD 774/5 and 993/4, *Nat. Commun.*, *6*, 8611, doi:10.1038/ncomms9611.
Miyake, F., K. Nagaya, K. Masuda, and T. Nakamura (2012), A signature of cosmic-ray increase in AD 774–775 from tree rings in Japan, *Nature*, *486*(7402), 240–242.
Owens, M. J., and R. J. Forsyth (2013), The Heliospheric Magnetic Field, *Living Rev. Sol. Phys.*, *10*, 5, doi:10.12942/lrsp-2013-5.
Owens, M. J., and M. Lockwood (2012), Cyclic loss of open solar flux since 1868: The link to heliospheric current sheet tilt and implications for the Maunder Minimum, *J. Geophys. Res.*, *117*, A04102, doi:10.1029/2011JA017193.
Owens, M. J., M. Lockwood, C. J. Davis, and L. Barnard (2011), Solar cycle 24: Implications for energetic particles and long-term space climate change, *Geophys. Res. Lett.*, *38*, L19106, doi:10.1029/2011GL049328.
Owens, M. J., I. Usoskin, and M. Lockwood (2012), Heliospheric modulation of galactic cosmic rays during grand solar minima: Past and future variations, *Geophys. Res. Lett.*, *39*, L19102, doi:10.1029/2012GL053151.
Owens, M. J., K. G. McCracken, M. Lockwood, and L. Barnard (2015), The heliospheric Hale cycle over the last 300 years and its implications for a "lost" late 18th century solar cycle, *J. Space Weather Space Clim.*, *5*, A30, doi:10.1051/swsc/2015032.
Owens, M. J., et al. (2016), Near-Earth heliospheric magnetic field intensity since 1750: 1. Sunspot and geomagnetic reconstructions, *J. Geophys. Res. Space Physics*, *121*, doi:10.1002/2016JA022529.
Parker, E. N. (1958), Dynamics of the interplanetary gas and magnetic fields, *Astrophys. J.*, *128*, 664–676.
Potgieter, M. (2013), Solar modulation of cosmic rays, *Living Rev. Sol. Phys.*, *10*, 3.
Reames, D. V. (1999), Particle acceleration at the Sun and in the heliosphere, *Space Sci. Rev.*, *90*(3–4), 413–491.
Riley, P., et al. (2015), Inferring the structure of the solar corona and inner heliosphere during the maunder minimum using global thermodynamic magnetohydrodynamic simulations, *Astrophys. J.*, *802*(2), 105, doi:10.1088/0004-637X/802/2/105.
Roth, R., and F. Joos (2013), A reconstruction of radiocarbon production and total solar irradiance from the Holocene ^{14}C and CO_2 records: implications of data and model uncertainties, *Clim. Past*, *9*(4), 1879–1909.
Sigl, M., J. R. McConnell, M. Toohey, M. Curran, S. B. Das, R. Edwards, E. Isaksson, K. Kawamura, S. Kipfstuhl, and K. Krüger (2014), Insights from Antarctica on volcanic forcing during the Common Era, *Nat. Clim. Change*, *4*(8), 693–697.
Simpson, J. A. (2000), The cosmic Ray nucleonic component: The invention and scientific uses of the neutron monitor-(Keynote lecture), *Space Sci. Rev.*, *93*, 11–32, doi:10.1023/A:1026567706183.
Solanki, S. K., M. Schüssler, and M. Fligge (2000), Evolution of the Sun's large-scale magnetic field since the Maunder minimum, *Nature*, *408*, 445–447, doi:10.1038/35044027.
Steinhilber, F., J. A. Abreu, J. Beer, and K. G. McCracken (2010), Interplanetary magnetic field during the past 9300 years inferred from cosmogenic radionuclides, *J. Geophys. Res.*, *115*, A01104, doi:10.1029/2009JA014193.
Steinhilber, F., et al. (2012), 9,400 years of cosmic radiation and solar activity from ice cores and tree rings, *Proc. Natl. Acad. Sci. U.S.A.*, *109*, 5967–5971, doi:10.1073/pnas.1118965109.
Svalgaard, L., and E. W. Cliver (2010), Heliospheric magnetic field 1835–2009, *J. Geophys. Res.*, *115*, A09111, doi:10.1029/2009JA015069.
Tans, P., A. De Jong, and W. Mook (1979), Natural atmospheric ^{14}C variation and the Suess effect, *Nature*, *280*(5725), 826–828, doi:10.1038/280826a0.
Usoskin, I. G. (2013), A history of solar activity over millennia, *Liv. Rev. Sol. Phys.*, *10*(3), doi:10.1016/j.jare.2012.11.001.

Usoskin, I. G., and G. A. Kovaltsov (2012), Occurrence of extreme solar particle events: assessment from historical proxy data, *Astrophys. J.*, *757*(1), 92.

Usoskin, I. G., K. Mursula, S. K. Solanki, M. Schüssler, and G. A. Kovaltsov (2002), A physical reconstruction of cosmic ray intensity since 1610, *J. Geophys. Res.*, *107*(A11), 1374, doi:10.1029/2002JA009343.

Usoskin, I. G., S. K. Solanki, G. A. Kovaltsov, J. Beer, and B. Kromer (2006), Solar proton events in cosmogenic isotope data, *Geophys. Res. Lett.*, *33*, L08107, doi:10.1029/2006GL026059.

Usoskin, I. G., K. Horiuchi, S. Solanki, G. A. Kovaltsov, and E. Bard (2009), On the common solar signal in different cosmogenic isotope data sets, *J. Geophys. Res.*, *114*, A03112, doi:10.1029/2008JA013888.

Usoskin, I., B. Kromer, F. Ludlow, J. Beer, M. Friedrich, G. Kovaltsov, S. Solanki, and L. Wacker (2013), The AD775 cosmic event revisited: the Sun is to blame, *Astron. Astrophys.*, *552*, L3.

Usoskin, I., et al. (2015), The Maunder minimum (1645–1715) was indeed a Grand minimum: A reassessment of multiple datasets, *Astron. Astrophys.*, *581*, A95, doi:10.1051/0004-6361/201526652.

Vieira, L. E. A., and S. K. Solanki (2010), Evolution of the solar magnetic flux on time scales of years to millenia, *Astron. Astrophys.*, *509*, A100, doi:10.1051/0004-6361/200913276.

Wang, Y.-M., J. Lean, and N. Sheeley Jr. (2005), Modeling the Sun's magnetic field and irradiance since 1713, *Astrophys. J.*, *625*(1), 522.

Webber, W., and P. Higbie (2003), Production of cosmogenic Be nuclei in the Earth's atmosphere by cosmic rays: Its dependence on solar modulation and the interstellar cosmic ray spectrum, *J. Geophys. Res.*, *108*(A9), 1355, doi:10.1029/2003JA009863.

Webber, W., P. Higbie, and K. McCracken (2007), Production of the cosmogenic isotopes ^{3}H, ^{7}Be, ^{10}Be, and ^{36}Cl in the Earth's atmosphere by solar and galactic cosmic rays, *J. Geophys. Res.*, *112*, A10106, doi:10.1029/2007JA012499.

Zhang, J., I. Richardson, D. Webb, N. Gopalswamy, E. Huttunen, J. Kasper, N. Nitta, W. Poomvises, B. Thompson, and C. C. Wu (2007), Solar and interplanetary sources of major geomagnetic storms ($Dst \leq -100$ nT) during 1996–2005, *J. Geophys. Res.*, *112*, A10102, doi:10.1029/2007JA012891.